# Study of neuronal gain in a conductance-based leaky integrate-and-fire neuron model with balanced excitatory and inhibitory synaptic input

A. N. Burkitt, H. Meffin, and D. B. Grayden
The Bionic Ear Institute, 384–388 Albert Street,
East Melbourne, Vic 3002, Australia

email: a.burkitt@medoto.unimelb.edu.au

**To appear in Biological Cybernetics**

**Abstract**

Neurons receive a continual stream of excitatory and inhibitory synaptic inputs. A conductance-based neuron model is used to investigate how the balanced component of this input modulates the amplitude of neuronal responses. The output spiking-rate is well-described by a formula involving three parameters: the mean $\mu$ and variance $\sigma$ of the membrane potential and the effective membrane time constant $\tau_{\rm Q}$. This expression shows that, for sufficiently small $\tau_{\rm Q}$, the level of balanced excitatory-inhibitory input has a non-linear modulatory effect on the neuronal gain.

## 1 Introduction

Gain modulation is a change in the amplitude of the response that a neuron generates in response to an additional stream of input (the modulatory one), but which does not affect the receptive field characteristics (or selectivity) of the neuron. It provides a non-linear mechanism by which information is combined between different pathways of neural processing, which may be of sensory, motor or cognitive origin. Gain modulation has been shown experimentally to play a role in sensory-motor integration, such as eye and reaching movements, and in spatial perception, as well as auditory masking, attentional processing, object recognition and navigation (Salinas & Thier, 2000). Experimental studies have established gain modulation as one of the important unifying computational principles in the brain, pervading multiple functions and brain areas (Salinas & Sejnowski, 2001).

Although experimental studies have shown gain modulation to play an important role in neural processing, our understanding of the underlying biophysical mechanisms by which neural systems implement gain modulation is lacking. The central question is: How do neurons achieve the non-linear, multiplicative behavior characteristic of gain modulation, when their input-output relationship is basically integrative? A number of possible different mechanisms have been proposed (Salinas & Thier, 2000): non-linear interactions in the dendritic processing of neurons (Mel, 1993), non-linear interactions arising from recurrent

connections between neurons (Salinas & Abbott, 1996; Hahnloser *et al.*, 1999), correlations in the synaptic input (Salinas & Sejnowski, 2000), and non-linear responses modulated by the balanced component of the synaptic input (Chance *et al.*, 2002).

This paper examines the mechanisms by which balanced synaptic input modulates neuronal gain. Balanced excitatory and inhibitory synaptic inputs have received particular attention recently (Shadlen & Newsome, 1994; Tsodyks & Sejnowski, 1995; van Vreeswijk & Sompolinsky, 1996; Troyer & Miller, 1997; Hohn & Burkitt, 2001), since the variability in the spike times of such models agrees well with that observed in cortical neurons (Softky & Koch, 1993; Shadlen & Newsome, 1994; Shadlen & Newsome, 1998). The possible role of balanced input in neuronal gain modulation was highlighted by a recent *in vitro* study in which a variable current (with zero mean) was injected into a rat cortical pyramidal neuron and the gain associated with the injection of an additional constant current was measured (Chance *et al.*, 2002). The results indicated that the variability of the injected current affected the neuronal gain multiplicatively. In this paper an analytic expression is derived for the output spiking-rate of a conductance-based integrate-and-fire neuron. This enables us to identify the conditions under which the output spiking-rate is modulated by the balanced input.

# 2 The conductance-based leaky integrate-and-fire neuron model

A one-compartment conductance-based leaky integrate-and-fire neuron is used in which the membrane potential $V(t)$ is the integrated activity of its excitatory and inhibitory synaptic inputs, and it decays in time with a characteristic time constant (Tuckwell, 1979; Tuckwell, 1989; Troyer & Miller, 1997; Salinas & Sejnowski, 2000; Tiesinga *et al.*, 2000; Destexhe *et al.*, 2001)

$$dV = -\frac{(V - v_0)}{\tau}dt + g_I(V_I - V)\,dP_I + g_E(V_E - V)\,(dP_E + dP_D). \quad (1)$$

The first term models the passive leak of the membrane, with resting potential $v_0$ and membrane time constant $\tau$. The second and third terms represent the synaptic contribution due to cortical background activity from excitatory ($dP_E$) and inhibitory ($dP_I$) neurons, respectively. In the balanced neuron considered here, the net contribution of the background activity is approximately zero because the average values of these excitatory and inhibitory terms are chosen to approximately cancel. In addition to the background activity, there is a synaptic driving current modelled as an excitatory fourth term ($dP_D$). The inputs $dP_E$, $dP_I$, $dP_D$ are independent temporally homogeneous Poisson processes with constant intensities $\gamma_E = N_E\lambda_E$, $\gamma_I = N_I\lambda_I$ and $\gamma_D = N_D\lambda_D$ respectively, i.e., each of the $N_E$ excitatory input fibers (resp. $N_I$ inhibitory, $N_D$ driving input fibers) has a spiking-rate $\lambda_E$ (resp. $\lambda_I$, $\lambda_D$). $V_E$ and $V_I$ are the (constant) reversal potentials ($V_I \leq v_0 \leq V(t) \leq V_{\rm th} < V_E$). The parameters $g_E$ and $g_I$ represent the integrated conductances over the time course of the synaptic event divided by the neural capacitance (and are thus dimensionless): they are nonnegative and are taken here to be identical for all excitatory and inhibitory inputs, respectively. When the membrane potential reaches a threshold $V_{\rm th}$, an output spike is generated and the membrane potential is reset to its resting value $v_0$.

In the absence of spike generation, the membrane potential approaches an equilibrium value, $\mu$, about which it fluctuates with variance $\sigma^2$. The membrane potential approaches $\mu$

with a time constant that is different from the passive membrane time constant due to the effect of the synaptic conductances, which is called the *effective* membrane time constant $\tau_{\rm Q}$. The values of $\mu$, $\sigma$, $\tau_{\rm Q}$ are (Hanson & Tuckwell, 1983; Burkitt, 2001)

$$\begin{aligned} \mu &= \frac{v_0/\tau + r_{11}}{1/\tau_{\rm Q}} \\ \sigma^2 &= \frac{\mu^2 r_{20} - 2\mu r_{21} + r_{22}}{2/\tau_{\rm Q} - r_{20}} \\ \frac{1}{\tau_{\rm Q}} &= \frac{1}{\tau} + r_{10} \\ r_{mn} &= (\gamma_E + \gamma_D) g_E^m V_E^n + \gamma_I g_I^m V_I^n. \end{aligned} \tag{2}$$

The analysis is carried out in the Gaussian approximation (Burkitt & Clark, 2000), in which the probability density of the membrane potential $p(v, t \,|\, v', 0)$ is parameterized as

$$p(v, t \,|\, v', 0) = \frac{1}{\sqrt{2\,\pi\,\Gamma(t; v')}} \, \exp\left\{ -\frac{(v - \Upsilon(t; v'))^2}{2\,\Gamma(t; v')} \right\}, \tag{3}$$

where $\Upsilon(t; v)$ and $\Gamma(t; v)$ are the (time-dependent) mean and variance of the membrane potential. The Gaussian approximation is accurate in the limit of a large number ($N$) of small amplitude synaptic inputs, which allows the probability density of the membrane potential to be evaluated using a self-consistent analysis (Burkitt, 2001). The output spike distribution $f_\theta(t)$ obeys the renewal equation (Plesser & Tanaka, 1997; Burkitt & Clark, 1999)

$$p(V_{\rm th}, t \,|\, v_0, 0) = \int_0^t dt' \, f_\theta(t') \, p(V_{\rm th}, t \,|\, V_{\rm th}, t'), \tag{4}$$

where $p(v, t \,|\, v', t')$ is the conditional probability density of the membrane potential having the value $v$ at time $t$, given that it had the value $v'$ at an earlier time $t'$ (this equation is exact when the synaptic current is modelled as a series of delta functions, otherwise it is approximate).

The output spiking-rate is determined from the average inter-spike interval

$$\lambda_{\rm out} = \left[ \tau_{\rm a} + \int_0^\infty t \, f_\theta(t) \, dt \right]^{-1}, \tag{5}$$

where $\tau_{\rm a}$ is the absolute refractory period (taken to be zero here). The above integral is evaluated using Laplace transforms, where the Laplace transform for $f_\theta(t)$ is obtained from Eq.(4) using the time-translation invariance $p(v, t \,|\, v', t') = p(v, t - t' \,|\, v', 0)$. The time-dependent mean and variance are given by (see Section 2.3 of (Burkitt, 2001))

$$\begin{aligned} \Upsilon(t; v_0) &= \mu \left( 1 - e^{-t/\tau_{\rm Q}} \right) \\ \Gamma(t; v_0) &= \sigma^2 \left( 1 - e^{-2t/\tau_{\rm Q}} \right) \quad , \end{aligned} \tag{6}$$

where $r_{20}$ is neglected in comparison with $r_{10}$ in the exponent of $\Gamma(t; v_0)$. Careful consideration of the finite and divergent parts of the resultant integrals gives the output spiking-rate, as shown in the Appendix,

$$\lambda_{\rm out}^{-1} = \frac{\tau_{\rm Q}}{\sigma} \sqrt{\frac{\pi}{2}} \int_{v_0}^{V_{\rm th}} du \, \exp\left( \frac{(u - \mu)^2}{2\sigma^2} \right) \left[ 1 + {\rm erf}\left( \frac{u - \mu}{\sigma\sqrt{2}} \right) \right]. \tag{7}$$

This is the so-called Siegert formula (Siegert, 1951; Ricciardi, 1977; Tuckwell, 1988; Amit & Tsodyks, 1991), but with the membrane time constant $\tau$ replaced by the effective time constant $\tau_{\rm Q}$. Note that once the parameters $V_{\rm th}$ and $v_0$ have been chosen, this formula gives the mean spiking-rate as a function of the three variables $\mu, \sigma$ and $\tau_{\rm Q}$, which are experimentally accessible (Inoue *et al.*, 1995; Destexhe & Paré, 1999).

# 3 Results

Background spiking activity in the cortex is reported to occur in the range of 5-20 Hz (Abeles, 1991). To investigate the effect of the level of background activity on the modulation of neuronal gain, '1.5X' and '2X' conditions were defined, corresponding to an increase by factors of 1.5 and 2, respectively, in the background activity (termed the '1X' condition). The 1X condition was defined by choosing parameters $\mu, \sigma$ and $\tau_{\rm Q}$ in Eq.(7) so that a spiking-rate of 5 Hz results from balanced background activity without a driving input. The effect upon neuronal gain was investigated by introducing driving input with spiking-rate $\gamma_D$.

An essential part of the analysis was defining the "normal operating regime" of a neuron, to ensure that the chosen parameter values correspond to biologically relevant neural behavior. The values of potentials were chosen to be $V_E = 0$mV, $V_I = -80$mV, $v_0 = -70$mV, $V_{\rm th} = -55$mV, and the passive membrane time constant was $\tau = 20$ms. These values accord with well-established measurements for cortical pyramidal neurons, and our results are not sensitive to variation of these potentials within the biologically plausible range. The experimentally accessible quantities $\mu, \sigma$ and $\tau_{\rm Q}$ (Destexhe & Paré, 1999) to be investigated were defined by first establishing appropriate ranges in the 1X condition without driving input. These were: $(\mu - v_0)/\theta \in [0.0, 1.0]$, $\sigma/\theta \in [0.01, 1.0]$ and $\tau_{\rm Q}/\tau \in [0.001, 1.0]$, where $\theta = V_{\rm th} - v_0$. A set of triplets $(\mu, \sigma, \tau_{\rm Q})$ were chosen that covered this region, with the constraint that their resultant output firing-rate was $\lambda_{\rm out} = 5$ Hz. For each triplet $\{(\mu, \sigma, \tau_{\rm Q}) \,|\, \lambda_{\rm out} = 5 \text{ Hz}\}$ the set of values of $g_E$, $g_I$, $\gamma_E$ and $\gamma_I$ that could give rise to the triplet were inferred from Eq.(2). An upper bound on $g_E$ was set by the requirement that at least 20 synaptic inputs were required for the neuron to reach threshold from the reset potential $v_0$ (and $g_E$, $g_I > 0$). Cortical neurons receive at least 1000 synaptic inputs and the spontaneous (input) spiking-rates $\lambda_E$, $\lambda_I$ have a lower bound of 1 Hz (Abeles, 1991). This procedure provided a finite space of parameters $g_E$, $g_I$, $\gamma_E$ and $\gamma_I$ capable of accounting for the range of plausible values $\mu$, $\sigma$ and $\tau_{\rm Q}$ in the 1X condition with no driving input. The 1.5X and 2X conditions were obtained by increasing the values of $\gamma_E$ and $\gamma_I$ appropriately.

To investigate how the level of balanced background activity affects neuronal gain, the output spiking-rate was plotted as a function of driving current in the 1X, 1.5X, and 2X conditions for the full range of biologically plausible parameters identified. The results revealed two qualitatively different behaviors (Fig. 1). The first type (Fig. 1a) was characterized by a linear response to driving input for all three conditions over most of the range of biologically relevant output spiking-rates (taken here to be 5-120 Hz). The figure shows some deviation from linearity in the 1X condition for low output spiking-rates (5-30 Hz). The effect of increased balanced background activity was simply to increase the spiking-rate by a fixed amount, independent of the driving spiking-rate $\gamma_D$. There was little effect on the gain, which remained approximately constant for all three conditions and most values of the driving spiking-rate (Fig. 1b). This type of behavior was expected when the equilibrium potential was above threshold. Remarkably, however, this behavior could occur even if the equilibrium potential was below threshold (see inset to Fig. 1a, showing $\mu$ and $\sigma$ relative to

$\theta$). The second type of behavior (Fig. 1e) also exhibited an additive effect on the output spiking-rate, but was further characterized by a non-linear response to driving input and a modulation in gain due to varying levels of background activity. Fig. 1e shows that in the absence of driving input, increases in the level of balanced background activity caused increased spiking-rates, as in the first type of behavior. However, there was a modulation of gain such that it decreased as the background activity increased (Fig. 1f). There was also intermediate behavior between these two types (Fig. 1c) in which the response to driving input was initially non-linear, but became linear as $\gamma_D$ increased. In this case there was a difference in the gain between the 1X and 2X conditions provided that the driving spiking-rate was not so high as to put the 2X condition into the linear regime. To a first approximation, the types of behavior may be well characterized according to the value of $\tau_{\rm Q}$. Given a biologically relevant range of output spiking-rates from 5 Hz (spontaneous activity) to 120 Hz (maximally driven output), linear behavior occurred across this entire range for $\tau_{\rm Q} \sim 20$ ms (the upper bound of $\tau_{\rm Q}$, since $\tau_{\rm Q} < \tau = 20$ ms for the parameters chosen here), while non-linear behavior with gain modulation occurred across the range if $\tau_{\rm Q} \leq 1$ms. For $1\text{ms} \leq \tau_{\rm Q} \leq 20\text{ms}$, intermediate behavior occurred: the cross-over point from linear to non-linear behavior (e.g., in Fig. 1a the linear regime was for $\lambda_{\rm out} > 30$ Hz) occurred at a value of $\lambda_{\rm out}$ that was inversely related to $\tau_{\rm Q}$. The gain modulation for values of $\tau_{\rm Q}$ less than $\sim 1$ ms, as illustrated in Fig. 1e,f, became more multiplicative-like when the spontaneous output spiking-rate (with $\gamma_D = 0$) was much lower than 5 Hz, as reported in (Chance *et al.*, 2002), but such low levels of spontaneous activity are outside the normal operating regime of cortical neurons. The change between linear and non-linear behavior also had some dependence upon the value of $\sigma$, which is discussed below.

Fig. 1 also shows the results of numerical simulations of the output spiking-rate (shown by triangles on the plots for the 1X condition). The numerical simulations were implemented by generating arrival times of the excitatory and inhibitory synaptic inputs according to Poisson distributions. The delta-function synaptic currents allow an exact update rule in which the membrane potential need only be evaluated at the synaptic input times. The results of numerical simulations show excellent agreement with those of the analytical expression for the parameters chosen here. The analytic expression for the output spiking-rate, Eq.(7), was derived by considering only terms up to second order in $g_E$ and $g_I$. Consequently this expression is most accurate for small values of these parameters (i.e., a large number of small amplitude synaptic inputs, where the amplitude is measured in relation to the difference between the reset and threshold potentials), which is the case for most of the biologically relevant parameter range.

All the results given above are essentially the same if the synaptic driving input, which is stochastic, is replaced by a steady injected current with the same value as the mean synaptic driving current: $I_D = C_m \gamma_D g_E (V_E - \mu)$, where $C_m$ is the capacitance per unit area of the membrane (taken to be $1\mu\text{F/cm}^2$). This is illustrated in Fig. 2, which shows data corresponding to Fig. 1e & 1f in the case of injected current. The results are nearly identical to those with synaptic driving input, indicating that the stochastic nature of the driving input $\gamma_D$ (but not the background input, $\gamma_E$, $\gamma_I$) was unimportant in the behavior described here. This is unsurprising since $\gamma_D \ll \gamma_E, \gamma_I$ and consequently the driving input contributes comparatively little to the fluctuations in the membrane potential.

To further understand the conditions that characterize the linear and non-linear behavior,

Eq.(5) was reparameterized as

$$\lambda_{\text{out}} \;=\; \frac{1}{\tau_{\text{Q}}}\, F\left(\frac{\mu - V_{\text{th}}}{\sqrt{2}\sigma}; \frac{\sigma}{\theta}\right) \;=\; \frac{1}{\tau_{\text{Q}}}\left[\int_{-\frac{(\mu - V_{\text{th}})}{\sqrt{2}\sigma} - \frac{\theta}{\sqrt{2}\sigma}}^{-\frac{(\mu - V_{\text{th}})}{\sqrt{2}\sigma}} du\, \sqrt{\pi}\, e^{u^2}\,(1 + \text{erf}u)\right]^{-1} \quad . \tag{8}$$

Fig. 3 shows that the function $F$ is approximately linear in the first argument provided that the argument is greater than $-c$, and is non-linear otherwise. The value of $c$ is in the range $[0.5, 1.5]$ depending on the strictness of the criteria for linearity and the ratio $\sigma/\theta$ (the smaller this ratio is, the larger the value of $c$). This result has two important implications. First, a linear input-output curve does not require that the mean membrane potential $\mu$ exceeds threshold, but rather that $\mu + \sqrt{2}c\sigma > V_{\text{th}}$. This provides a first criterion to determine whether gain modulation is present, since it specifies when the non-linear behavior occurs. Second, the transition from linear to non-linear behavior occurs when the output spiking-rate becomes larger than $\lambda^*_{\text{out}} = F(-c, \sigma/\theta)/\tau_{\text{Q}}$, where $0.07 \leq F(-c, \sigma/\theta) \leq 0.3$, as illustrated in Fig. 3b. This provides a second criterion for the presence of gain modulation behavior that relates directly to the output spiking-rate. For example, a value of $c$ in the middle of this range ($F(-c, \sigma/\theta) \approx 0.12$) produces linear behavior over the range $\lambda_{\text{out}}$ =5-120 Hz for $\tau_{\text{Q}} \geq$ 20ms and non-linear behavior for $\tau_{\text{Q}} \leq$ 1ms, consistent with the above observation. These limiting values of $\tau_{\text{Q}}$, for which purely linear or purely non-linear behavior occurs, increase as $\sigma/\theta$ increases, because this gives a smaller value of $c$ that in turn produces a larger value of $F(-c, \sigma/\theta)$ (see Fig. 3a).

# 4 Discussion and Conclusions

The effect upon gain modulation of increasing the balanced background activity can be understood in terms of two competing processes embodied in Eq.(8), both influenced by the effective membrane time constant, $\tau_{\text{Q}}$. First, the contribution of a driving input to the mean membrane potential, $\mu_D$, is approximately linear in $\gamma_D$, namely $\mu_D = \gamma_D g_E \tau_{\text{Q}} V_E$ from Eq.(2). As the level of background activity increases, the effective time constant, $\tau_{\text{Q}}$, decreases, resulting in a lower value of $\mu$ for a given driving spiking-rate, $\gamma_D$. This decrease in $\tau_{\text{Q}}$ is due to the neuron becoming more leaky as more synaptic channels open (Tiesinga *et al.*, 2000). The value of $\sigma$ remains approximately constant for all conditions and driving spiking-rates, also as a result of the increased leakiness. Although lower values of $\mu$ are expected to decrease the output spiking-rate, this is offset by a second effect: the neuron operates on a faster time scale as $\tau_{\text{Q}}$ decreases, and so the time course and fluctuations in the membrane potential are more rapid. From Eq.(8), when the neuron is in the linear regime these two competing effects approximately cancel and there is no gain modulation. When the neuron is in the non-linear regime the effect of the extra leakiness dominates over the effect of the faster time scale, resulting in diminished gain as the level of background activity increases.

The relative strength of these two opposing effects in different parameter regions explains many of the the differing results on gain modulation reported by a number of authors (Nelson, 1994; Carandini & Heeger, 1994; Holt & Koch, 1997; Tiesinga *et al.*, 2000; Capaday, 2002; Longtin *et al.*, 2002; Chance *et al.*, 2002). The lack of gain modulation in the linear regime was first noted by (Holt & Koch, 1997), and a recent study of motoneurons (Capaday, 2002) showed no gain modulation, since they operate in the linear regime. The explanation of the linear behavior in these papers is based upon approximating the spiking-rate by the inverse

of the mean time taken for the membrane potential to reach threshold when only the mean input is considered (i.e., the stochastic nature of the changes to the membrane potential is ignored). When the membrane fluctuations are incorporated, this approximation remains valid only if the equilibrium membrane potential, $\mu$ (Eq. 2), is close to or above the spiking threshold. As the discussion following Eq.(8) indicates, such models correspond to the linear regime of the function $F$ where no gain modulation is observed. The analysis presented here provides a quantitative prediction of the parameter regime in which the balanced component of the synaptic input gives rise to non-linear gain modulation of the spiking-rate and indicates that such conditions are within the biologically plausible region of cortical neurons.

The distinction between the signal input and the background (modulatory) input is based not upon any anatomical difference, but rather upon the particular function that the synaptic input plays. For neurons in the non-linear regime, the results here indicate that higher levels of balanced excitation and inhibition will produce a lower response gain in the output spiking-rate of the neuron. Important questions that remain include whether a balance of excitatory and inhibitory synaptic input exists *in vivo*, whether the level of balanced input can be modulated in a behaviorally functional way, and whether such balanced synaptic input arises from feedforward, recurrent or feedback networks. Indirect evidence for balanced synaptic input *in vivo* is provided by the irregular spiking of cortical neurons (Shadlen & Newsome, 1994). The large observed values of the coefficient of variation of the interspike interval distribution is inconsistent with the integration of a large number of small amplitude postsynaptic potentials (Softky & Koch, 1993) unless the neurons receive roughly balanced amounts of excitatory and inhibitory synaptic input (Shadlen & Newsome, 1998). The question of whether such balanced input can be modulated in a functionally significant way in cortical neurons is much less clear. Indirect experimental support for a feedback source of balanced synaptic input is provided by studies on the primary visual cortex of monkeys in response to drifting grating stimuli, in which the contrast, orientation and spatiotemporal frequencies were varied (Carandini & Heeger, 1994). The analysis presented here provides a neural mechanism for the non-linear response observed in these studies, without the need for the proposed "normalization" synaptic conductances that were postulated in their normalization model of gain modulation (in which a non-linear neural response is generated by the interaction of a neuron with the pooled activity of a large number of nearby neurons) (Carandini & Heeger, 1994). More recent models of gain modulation have also used recurrent and feedback interactions (Salinas & Abbott, 1996; Hahnloser *et al.*, 1999).

In conclusion, the results presented here give a quantitative picture of the extent to which neuronal gain can be modulated by the balanced component of the synaptic input for neurons with biologically realistic parameters. This analysis highlights the role played by the effective time constant, $\tau_{\mathrm{Q}}$, which results from the increased leakiness of the membrane as the balanced synaptic input increases (Tiesinga *et al.*, 2000). Consequently, increases in the variance of the synaptic input do not necessarily cause corresponding increases in the variance of the membrane potential. The effect of gain modulation becomes most pronounced for $\tau_{\mathrm{Q}}$ less than approximately 1 ms, where increased levels of background activity produce a lower neural gain over most of the output spiking-rate range. Therefore, it is in this region that the gain modulation produced by the balanced synaptic input will potentially have the greatest functional significance, although the boundary of the region will depend upon the ratio $\sigma/\theta$.

# Appendix

## A Derivation of the Siegert Formula

In this appendix the Siegert formula is derived for the leaky integrate-and-fire neuron with reversal potentials in the Gaussian approximation. The renewal equation (4) may be solved for the first-passage time density, $f_\theta(t)$, using Laplace transforms,

$$f_{\rm L}(s) = \frac{p_{\rm L}(s)}{q_{\rm L}(s)}\,, \tag{9}$$

where the subscript $L$ denotes the Laplace transform and $p_L(s)$ and $q_L(s)$ are the Laplace transforms of the probability density of the membrane potential, $p(v,t|v',0)$:

$$p_{\rm L}(s) = \int_0^\infty dt\, e^{-st}\, p(V_{\rm th},t|v_0,0), \tag{10}$$

$$q_{\rm L}(s) = \int_0^\infty dt\, e^{-st}\, p(V_{\rm th},t|V_{\rm th},0). \tag{11}$$

Using (5) the mean firing rate can be calculated from the mean ISI, $t_f$, given by

$$t_f = \int_0^\infty t\, f_\theta(t)\, dt = \frac{p_{\rm L}(0)\, q'_{\rm L}(0) - p'_{\rm L}(0)\, q_{\rm L}(0)}{q_{\rm L}(0)\, p_{\rm L}(0)}. \tag{12}$$

The integrals in (10) & (11) and their derivatives can be re-written using the Gaussian approximation for $p(v,t|v',0)$ (Eqns.(3) & (7)) with the change of variable $x = \exp(-t/\tau_{\rm Q})$

$$\frac{d^n}{ds^n} p_{\rm L}(s) = \int_0^1 dx (\tau_{\rm Q} \ln x)^n \frac{\tau_{\rm Q} x^{\tau_{\rm Q} s-1}}{\sqrt{2\pi\sigma^2(1-x^2)}} \exp\left\{-\frac{(y_{\rm th}-y_{\rm r}x)^2}{1-x^2}\right\}, \tag{13}$$

$$\frac{d^n}{ds^n} q_{\rm L}(s) = \int_0^1 dx (\tau_{\rm Q} \ln x)^n \frac{\tau_{\rm Q} x^{\tau_{\rm Q} s-1}}{\sqrt{2\pi\sigma^2(1-x^2)}} \exp\left\{-\frac{y_{\rm th}^2(1-x)^2}{1-x^2}\right\}, \tag{14}$$

where $y_{\rm th} = \frac{V_{\rm th}-\mu}{\sqrt{2}\sigma}$, $y_{\rm r} = \frac{v_0-\mu}{\sqrt{2}\sigma}$. In the limit as $s \to 0$ these integrals are divergent (the integrand is singular at $x = 0$) and can be written in terms of finite and singular parts

$$\frac{d^n}{ds^n} p_{\rm L}(s) = \frac{\tau_{\rm Q}}{\sqrt{2\pi\sigma^2}} \left[ p_{\rm F}(s;n) + \frac{(-1)^n n! \exp(-y_{\rm th}^2)}{\tau_{\rm Q} s^{n+1}} \right], \tag{15}$$

$$\frac{d^n}{ds^n} q_{\rm L}(s) = \frac{\tau_{\rm Q}}{\sqrt{2\pi\sigma^2}} \left[ q_{\rm F}(s;n) + \frac{(-1)^n n! \exp(-y_{\rm th}^2)}{\tau_{\rm Q} s^{n+1}} \right], \tag{16}$$

where $p_{\rm F}(s;n)$ and $q_{\rm F}(s;n)$ are the finite parts of $p_{\rm L}(s)$ and $q_{\rm L}(s)$ respectively,

$$p_{\rm F}(s;n) = \int_0^1 dx (\tau_{\rm Q}\, \ln x)^n \frac{x^{\tau_{\rm Q} s-1}}{\sqrt{(1-x^2)}} \left[ \exp\left\{-\frac{(y_{\rm th}-y_{\rm r}x)^2}{1-x^2}\right\} - \exp(-y_{\rm th}^2)\sqrt{(1-x^2)} \right], \tag{17}$$

$$q_{\rm F}(s;n) = \int_0^1 dx (\tau_{\rm Q}\, \ln x)^n \frac{x^{\tau_{\rm Q} s-1}}{\sqrt{(1-x^2)}} \left[ \exp\left\{-\frac{y_{\rm th}^2(1-x)^2}{1-x^2}\right\} - \exp(-y_{\rm th}^2)\sqrt{(1-x^2)} \right]. \tag{18}$$

In (12) for the mean ISI, the singular parts cancel so that in the limit as $s \to 0$

$$t_f = \exp(y_{\rm th}^2)\left(\int_0^1 dx \frac{\tau_{\rm Q} x^{-1}}{\sqrt{(1-x^2)}} \exp\left\{-\frac{y_{\rm th}^2(1-x)^2}{1-x^2}\right\} - \int_0^1 dx \frac{\tau_{\rm Q} x^{-1}}{\sqrt{(1-x^2)}} \exp\left\{-\frac{(y_{\rm th}-y_{\rm r}x)^2}{1-x^2}\right\}\right). \tag{19}$$

Consider these two integrals separately and notice that the following related identities hold:

$$\frac{d}{du}\left[\exp(u^2)\int_0^1 dx \frac{x^{-1}}{\sqrt{(1-x^2)}}\left\{\exp\left(-\frac{u^2(1-x)^2}{1-x^2}\right) - \exp\left(-u^2\right)\right\}\right] = 4\exp(u^2)\int_0^u dz \exp(-z^2), \tag{20}$$

$$\frac{d}{du}\left[\exp(u^2)\int_0^1 dx \frac{x^{-1}}{\sqrt{(1-x^2)}}\left\{\exp\left(-\frac{(u-y_{\rm r}x)^2}{1-x^2}\right) - \exp\left(-u^2\right)\right\}\right] = -2\exp(u^2)\int_u^\infty dz \exp(-z^2). \tag{21}$$

Consequently,

$$\begin{aligned} t_f &= \tau_{\rm Q}\int_{y_{\rm r}}^{y_{\rm th}} du\, \exp(u^2)\left(4\int_0^u dz \exp(-z^2) + 2\int_u^\infty dz \exp(-z^2)\right) \\ &= \tau_{\rm Q}\int_{y_{\rm r}}^{y_{\rm th}} du\, \exp(u^2)\left(2\left[\int_0^\infty dz \exp(-z^2) + \int_0^u dz \exp(-z^2)\right]\right) \\ &= \sqrt{\pi}\tau_{\rm Q}\int_{\frac{v_0-\mu}{\sqrt{2}\sigma}}^{\frac{V_{\rm th}-\mu}{\sqrt{2}\sigma}} du\, \exp(u^2)\left[1+\mathrm{erf}(u)\right] \\ &= \frac{\tau_{\rm Q}}{\sigma}\sqrt{\frac{\pi}{2}}\int_{v_0}^{V_{\rm th}} du\, \exp\left(\frac{(u-\mu)^2}{2\sigma^2}\right)\left[1+\mathrm{erf}\left(\frac{u-\mu}{\sqrt{2}\sigma}\right)\right]. \end{aligned} \tag{22}$$

# Acknowledgments

This work was funded by the Australian Research Council (ARC Discovery Project #DP0211972) and The Bionic Ear Institute. We thank an anonymous reviewer for useful comments on the manuscript.

# References

Abeles, M. 1991. *Corticonics: Neural Circuits of the Cerebral Cortex*. New York: Cambridge University Press.

Amit, D. J., & Tsodyks, M. V. 1991. Quantitative Study of Attractor Neural Network Retrieving at Low Spike Rates: I. Substrate - Spikes, Rates and Neuronal Gain. *Network: Comput. Neur. Sys.*, **2**, 259–273.

Burkitt, A. N. 2001. Balanced Neurons: Analysis of Leaky Integrate-and-Fire Neurons with Reversal Potentials. *Biol. Cybern.*, **85**, 247–255.

Burkitt, A. N., & Clark, G. M. 1999. Analysis of Integrate-and-Fire Neurons: Synchronization of Synaptic Input and Spike Output in Neural Systems. *Neural Comput.*, **11**, 871–901.

Burkitt, A. N., & Clark, G. M. 2000. Calculation of Interspike Intervals for Integrate-and-Fire Neurons with Poisson Distribution of Synaptic Inputs. *Neural Comput.*, **12**, 1789–1820.

Capaday, C. 2002. A Re-Examination of the Possibility of Controlling the Firing Rate Gain of Neurons by Balancing Excitatory and Inhibitory Conductances. *Exp. Brain Res.*, **143**, 67–77.

Carandini, M., & Heeger, D. J. 1994. Summation and Division by Neurons in Primate Visual Cortex. *Science*, **264**, 1333–1336.

Chance, F. S., Abbott, L. F., & Reyes, A. D. 2002. Gain Modulation from Background Synaptic Input. *Neuron*, **35**, 773–782.

Destexhe, A., & Paré, D. 1999. Impact of Network Activity on the Integrative Properties of Neocortical Neurons in Vivo. *J. Neurophysiol.*, **81**, 1531–1547.

Destexhe, A., Rudolph, M., Fellous, J-M., & Sejnowski, T. J. 2001. Fluctuating Synaptic Conductances Recreate *in-vivo*-Like Activity in Neocortical Neurons. *Neurosci.*, **107**, 13–24.

Hahnloser, R., Douglas, R. J., Mahowald, M., & Hepp, K. 1999. Feedback Interactions Between Neuronal Pointers and Maps for Attentional Processing. *Nature Neurosci.*, **2**, 746–752.

Hanson, F. B., & Tuckwell, H. C. 1983. Diffusion Approximations for Neuronal Activity Including Synaptic Reversal Potentials. *J. Theoret. Neurobiol.*, **2**, 127–153.

Hohn, N., & Burkitt, A. N. 2001. Shot noise in the leaky integrate-and-fire neuron. *Phys. Rev. E*, **63**, 031902.

Holt, G. R., & Koch, C. 1997. Shunting Inhibition does not have a Divisive Effect on Firing Rates. *Neural Comput.*, **9**, 1001–1013.

Inoue, J., Sate, S., & Ricciardi, L. M. 1995. On the Parameter Extimation for Diffusion Models of Single Neuron's Activities. *Biol. Cybern.*, **73**, 209–221.

Longtin, A., Doiron, B., & Bulsara, A. R. 2002. Noise Induced Divisive Gain Control in Neuron Models. *BioSys.*, **67**, 147–156.

Mel, B. W. 1993. Synaptic Integration in an Excitable Dendritic Tree. *J. Neurophysiol.*, **70**, 1086–1101.

Nelson, M. E. 1994. A Mechanism for Neuronal Gain Control by Descending Pathways. *Neural Comput.*, **6**, 242–254.

Plesser, H. E., & Tanaka, S. 1997. Stochastic Resonance in a Model Neuron with Reset. *Phys. Lett. A*, **225**, 228–234.

Ricciardi, L. M. 1977. *Diffusion Processes and Related Topics in Biology.* Berlin: Springer.

Salinas, E., & Abbott, L. F. 1996. A Model of Multiplicative Neural Response in Parietal Cortex. *Proc. Natl. Acad. Sci. USA*, **93**, 6461–6474.

Salinas, E., & Sejnowski, T. J. 2000. Impact of Correlated Synaptic Input on Output Firing Rate and Variability in Simple Neuronal Models. *J. Neurosci.*, **20**, 6193–6209.

Salinas, E., & Sejnowski, T. J. 2001. Gain Modulation in the Central Nervous System: Where Behavior, Neurophysiology and Computation Meet. *The Neuroscientist*, **7**, 430–440.

Salinas, E., & Thier, P. 2000. Gain Modulation: A Major Computational Principle of the Central Nervous System. *Neuron*, **27**, 15–21.

Shadlen, M. N., & Newsome, W. T. 1994. Noise, Neural Codes and Cortical Organization. *Curr. Opin. Neurobiol.*, **4**, 569–579.

Shadlen, M. N., & Newsome, W. T. 1998. The Variable Discharge of Cortical Neurons: Implications for Connectivity, Computation, and Information Coding. *J. Neurosci.*, **18**, 3870–3896.

Siegert, A. J. F. 1951. On the First Passage Time Probability Problem. *Phys. Rev.*, **81**, 617–623.

Softky, W. R., & Koch, C. 1993. The Highly Irregular Firing of Cortical Cells Is Inconsistent with Temporal Integration of Random EPSPs. *J. Neurosci.*, **13**, 334–350.

Tiesinga, P. H. E., José, J. V., & Sejnowski, T. J. 2000. Comparison of Current-Driven and Conductance-Driven Neocortical Model Neurons with Hodgkin-Huxley Voltage-Gated Channels. *Phys. Rev. E*, **62**, 8413–8419.

Troyer, T. W., & Miller, K. D. 1997. Physiological Gain Leads to High ISI Variability in a Simple Model of a Cortical Regular Spiking Cell. *Neural Comput.*, **9**, 971–983.

Tsodyks, M. V., & Sejnowski, T. J. 1995. Rapid State Switching in Balanced Cortical Network Models. *Network: Comput. Neural Sys.*, **6**, 111–124.

Tuckwell, H. C. 1979. Synaptic Transmission in a Model for Stochastic Neural Activity. *J. theor. Biol.*, **77**, 65–81.

Tuckwell, H. C. 1988. *Introduction to Theoretical Neurobiology: Volume 2, Nonlinear and Stochastic Theories*. Cambridge: Cambridge University Press.

Tuckwell, H. C. 1989. *Stochastic Processes in the Neurosciences*. Philadelphia: Society for Industrial and Applied Mathematics.

van Vreeswijk, C., & Sompolinsky, H. 1996. Chaos in Neuronal Networks with Balanced Excitatory and Inhibitory Activity. *Science*, **274**, 1724–1726.

# Figure Captions

Figure 1: Plots of the neuronal gain: Plots on left show output spiking-rate, $\lambda_{\rm out}$ Eq.(5), vs spiking-rate of driving inputs $\gamma_D$ for three typical sets of neural parameters, and plots on right show the corresponding gain vs $\gamma_D$. Results are shown for the 1X (solid line), 1.5X (dashed line) and 2X (dot-dashed line) conditions. The results of numerical simulations in the 1X condition with 10,000 output spikes are plotted as triangles. The insets in the left column show the corresponding values of $\mu$ (upper solid line) and $\sigma$ (lower solid line), as well as the spiking threshold (dotted line), vs $\gamma_D$ for the 1X condition (same range as corresponding larger plot in each case). Parameter values for the 1X condition are (a),(b) $g_E = 0.0027$, $g_I = 0.0092$, $\gamma_E = 21.6$ kHz, $\gamma_I = 15.4$ kHz, (i.e. $\tau_{\rm Q} = 4$ ms), (c),(d) $g_E = 0.0026$, $g_I = 0.0080$, $\gamma_E = 62.9$ kHz, $\gamma_I = 56.4$ kHz, (i.e. $\tau_{\rm Q} = 1.5$ ms),and (e),(f) $g_E = 0.0026$, $g_I = 0.0079$, $\gamma_E = 143$ kHz, $\gamma_I = 137$ kHz (i.e. $\tau_{\rm Q} = 0.67$ ms). Remaining neural parameter values are given in the text.

Figure 2: Plots of neuronal gain for steady injected current $I_D = C_m \gamma_D g_E (V_E - \mu_{1X})$ with parameters as for Fig. 1e & 1f. $C_m = 1\mu$F/cm$^2$ is the capacitance of the neural membrane and $\mu_{1X}$=-60.175mV is the mean membrane potential in the 1X condition without any driving input. (a) The output spiking-rate, $\lambda_{\rm out}$ Eq.(5), vs $I_D$ for three typical sets of neural parameters, and (b) the corresponding gain vs $I_D$. Results are shown for the 1X (solid line), 1.5X (dashed line) and 2X (dot-dashed line) conditions.

Figure 3: (a) The function $F$, Eq.(8), and (b) its derivative with respect to its first argument $x = \frac{\mu - V_{\rm th}}{\sqrt{2}\sigma}$ for several values of its second argument $\sigma/\theta = 0.05$ (solid), 0.1 (dashed) and 0.2 (dot-dashed). The vertical dotted lines in (b) illustrate the region $-1.5 \leq x \leq -0.5$ in which a transition from non-linearity to linearity occurs, depending on the values of $\sigma/\theta$ and the strictness of the criteria for linearity. The dotted lines in (a) give the corresponding region and values of the function $F$.

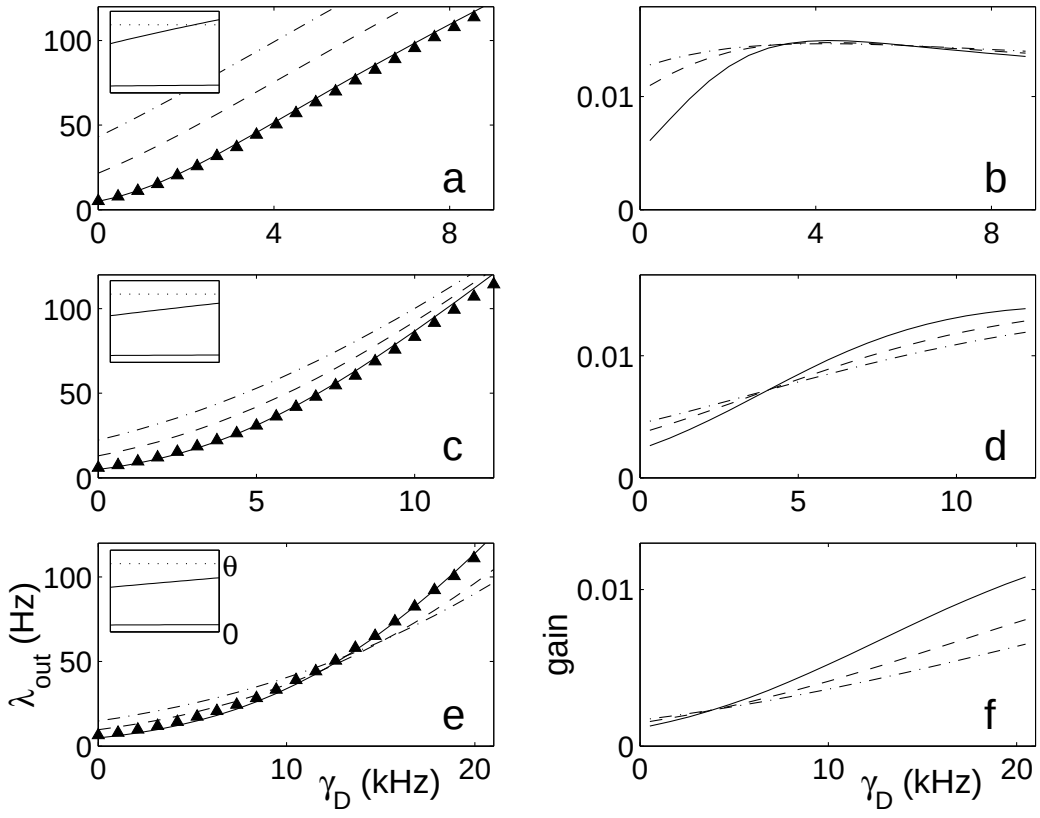


Figure 1:

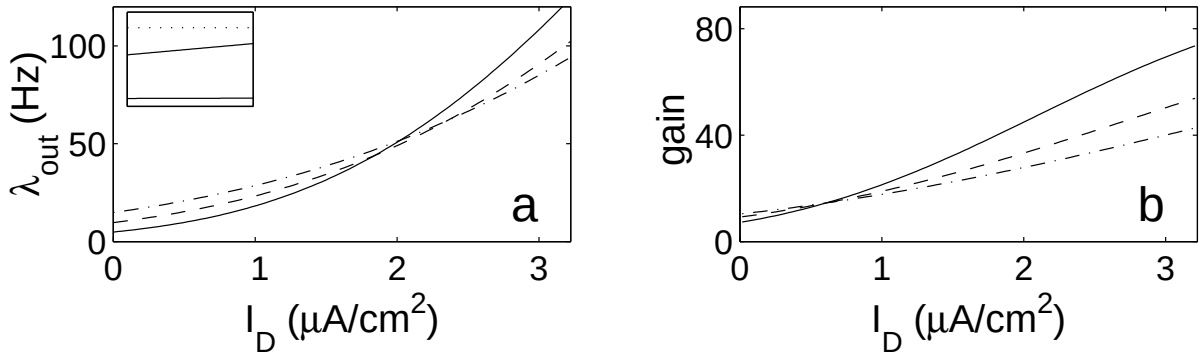


Figure 2:

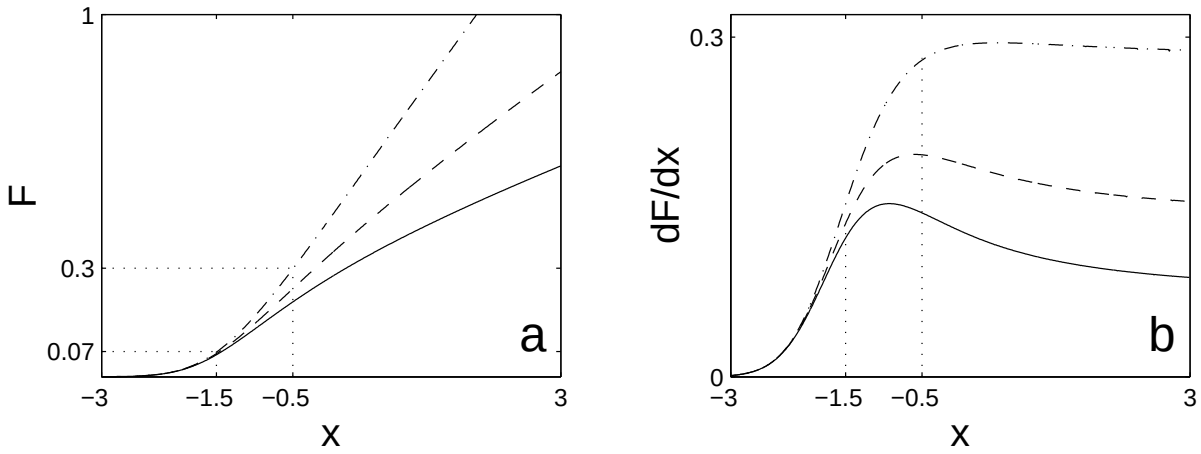


Figure 3: